COLD SPRAY TECHNOLOGY FOR STRUCTURAL RESTORATION OF SEA-BASED AVIATION STRUCTURAL MATERIALS

Saravanan R. Arunachalam and Sarah E. Galyon Dorman

SAFE Inc.
3290 Hamal Cir
Monument, CO 80132/USA

ABSTRACT

Additive manufacturing and thermal spray technologies are slowly transitioning to the Department of Defense as a method for restoring or manufacturing of obsolete or worn out parts. Specifically, among all thermal spray technologies, cold spray (CS) has proved to be an effective geometric restoration method which has the potential to repair, restore and enhance the airworthiness of aging aircraft. In general, CS involves the introduction of metallic powders (5 - 45 μm) into a gas stream and subsequently accelerated to a velocity range of 450 - 1200 meters/second. The powder particles that exit the nozzle impact the substrate in a solid state creating mechanical or mechanical/metallurgical bond depending on the substrate and the process parameters. Recently the Federal Aviation Administration (FAA) approved CS for dimensional repair of several non-structural aircraft parts. This research, focuses on a Office of Naval Research funded program to examine the CS technology qualification and approval process for repair and restoration of corrosion damage specifically for aircraft structural components. The paper provides preliminary results on microstructure evaluation, mechanical properties and galvanic corrosion studies on a 7075 Al plate repaired using CS technology.

1. INTRODUCTION

1.1 CS Process

Cold Spray (CS) also known as supersonic particle deposition (SPD), cold gas dynamic spraying, or kinetic energy metallization, is an additive manufacturing technology. During the CS process, micron-sized powder particles are accelerated to supersonic speed prior to impacting a substrate to form a solid-state deposit. Because the CS process normally operates below the melting point of the powder metals, it can deposit thermally and oxygen-sensitive aircraft materials such as aluminum and titanium alloys with less material degradation. Although CS has been used for geometric restoration of corrosion damaged components, its potential to repair the structural strength of load-bearing components with fatigue or corrosion damage has not been fully developed. Nor has the certification approach for these parts been defined. Many reviews of the CS process have been completed typically focusing on applicable material systems, future perspectives and new applications [1-2]. Applications of the SPD process for protective coatings and dimensional restoration have also been cited extensively in the literature [3-12].

SAMPE Conference Proceedings. Charlotte, NC, May 20-23, 2019. Society for the Advancement of Material and Process Engineering – North America.

1.2 Structural repair application

This program is aimed at providing the path towards obtaining a Department of Defense (DoD) acceptance strategy for CS repair. Early results for some of the mechanical and corrosion studies are also reported. In order to demonstrate the viability of CS repair for structural repair application, mechanical and chemical equivalencies of the CS with respect to the pristine material need to be evaluated at the coupon level, followed by part level testing. In addition, for the CS process specifically, the spray parameters need to be optimized and controlled to characterize spray material properties.

1.2.1 Mechanical Properties

Key mechanical properties for CS repair of aircraft parts are tensile, fatigue and bearing, in addition to coating characteristics such as percentage porosity, hardness and shear strength from triple-lug shear testing. Adhesion strength of the CS coating is often evaluated and reported in the literature, however this is not critical property. Meaning, the adhesive strength reported is truly not representative of the coating characteristics based on the type of test, whether it is a glue bond or glueless bond. In the case of glued bond testing, the measured strength is dictated by the strength of the glue. Thus, in this case it can be only used as pass fail criteria and not as a design property. Whereas, in the case of the glueless bond test, the coating thickness is not representative of repair thickness. The microstructural characteristics of CS vary with thickness of the coating, thus, the strength determined during glueless bond testing does not represent adhesion strength of the repair. While adhesion strength represents the quality of the coating, tensile, fatigue, bearing and fracture toughness are key design properties for structural repair applications. Thus, measured mechanical properties of CS repaired coupons will provide critical results on the CS coating quality and the mechanical equivalency of the CS repair to the base alloy.

1.2.2 Chemical Equivalency

The corrosion characteristics of CS are complicated and need a thorough understanding. Often, ASTM B117 (salt fog) test and open circuit potential measurement values are reported for CS [13]. However, in order to evaluate the corrosion characteristics, a comprehensive understanding of the galvanic behavior of the CS-substrate couple needs to be assessed. A schematic of galvanic couple often encountered during a CS repair is shown in Figure 1.

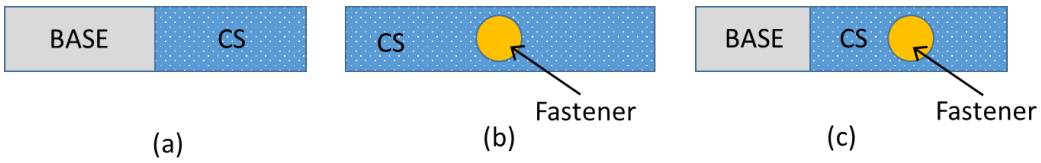

Figure 1. Schematic showing galvanic couple for a CS repair. (a) CS versus Base (substrate), (b) CS versus fastener and (c) CS versus fastener and base couples.

The schematic shown in Figure 1a represents a surface repair, "b" represents fastener repair and "c" represents effect of multi-element, i.e. CS-fastener-base. Thus, for CS chemical equivalency characteristics, a comprehensive study should include ASTM B117, galvanic current measurements for the different couples using ASTM G71, and exfoliation corrosion evaluation of galvanic couples using ASTM G34 [13, 14, 15].

The primary goal of this program is to determine the mechanical and chemical equivalency of a CS repair process using helium as carrier gas and to determine the feasibility for a structural repair for a sea-based aircraft application using 7XXX series aluminum alloys. As this program is in the preliminary stages, the present paper provides experimental results from a similar CS-repair process using nitrogen as carrier gas examined as part of this program. Specifically, corrosion evaluation of the CS using open circuit potential, galvanic current measurement and exfoliation corrosion evaluations for different CS-substrate couples are presented below.

2. EXPERIMENTATION

2.1 Material

In this study simulated corrosion damage was produced and repaired using CS. Aluminum alloy (AA) 7075-T651 6.35mm (0.25 inch) plate was used as a substrate material for the structural repair simulation and 44 μm (average particle size) aluminum (Al) 7075 gas atomized powder was used for the CS coating. The study involved simulating a 20% thickness loss by milling an AA 7075 plate. The plate was then repaired to the original dimensions using the CS process. Coatings were produced using commercially available helium gas atomized 7075 Al powder (Valimet, Stockton, CA, USA), 44 μm in size, deposited on milled plates and sheets use a VRC Gen III commercial CS system.

2.2 Microstructure Evaluation

AA 7075CS coating was analyzed by taking a cross section of the CS. The quality of the CS was assessed by measuring the average porosity from at least five different locations. Hardness of the coating was characterized using a Shimadzu nano-hardness tester. Extensive microstructure characterization was carried out to understand the cold sprayed coating using both optical and scanning electron (SEM) microscopes. Samples were polished using standard metallographic techniques and etched using Keller's reagent.

2.3 Corrosion Studies

Open circuit potential and galvanic current measurement of the CS were evaluated using a Gamry 3000 potentiostat instrument in a 1 M sodium chloride (NaCl) electrolyte. Both CS and substrate (base material) were cut to a square of 1 cm x 1 cm (thickness 6.35 mm (0.25 inch) for base and CS repaired specimens). The samples were mounted in clear acrylic and polished. The polished samples were given electrical contact using pure aluminum wire. The aluminum wires were then masked so only the polished sample surface was exposed to electrolyte. For galvanic corrosion measurements using ASTM G34 the following material combinations were used [15].

a) Base vs Base
b) Base vs CS
c) Base vs Titanium (Ti-6Al-4V)

d) Base vs Stainless steel (SS 304)
e) CS vs Titanium (Ti-6Al-4V)
f) CS vs Stainless Steel (SS 304)

Exfoliation corrosion studies were performed as per the schematic described in Figure 1. Ti-6Al-4V and 304 stainless steel fasteners (SS304) were used in the galvanic couple in addition to base and CS couple alone. A macrophotograph of the Ti-6Al-4V fastener joint for Base, CS, and Base-CS is shown in Figure 2. Visual as well as metallographic cross section examinations were carried out to characterize the corrosion behavior of the exfoliation solution (EXCO) exposed samples. The EXCO solution was prepared by dissolving 234 grams (g) of NaCl, 50 g of KNO_3 and 6.3 mL of concentrated HNO_3 (70 weight %) [14]. This solution was diluted to 1 liter (L) with deionized water. The pH of the solution was approximately 0.4 pH verified using pH paper [14]. All test coupons were placed in this EXCO solution and the temperature of the bath was maintained at 25 ± 3°C for a minimum of 1 hour prior to starting the exposures. All coupons were exposed to EXCO solution for 48 h, an exposure period recommended for 7XXX series aluminum alloys [14].

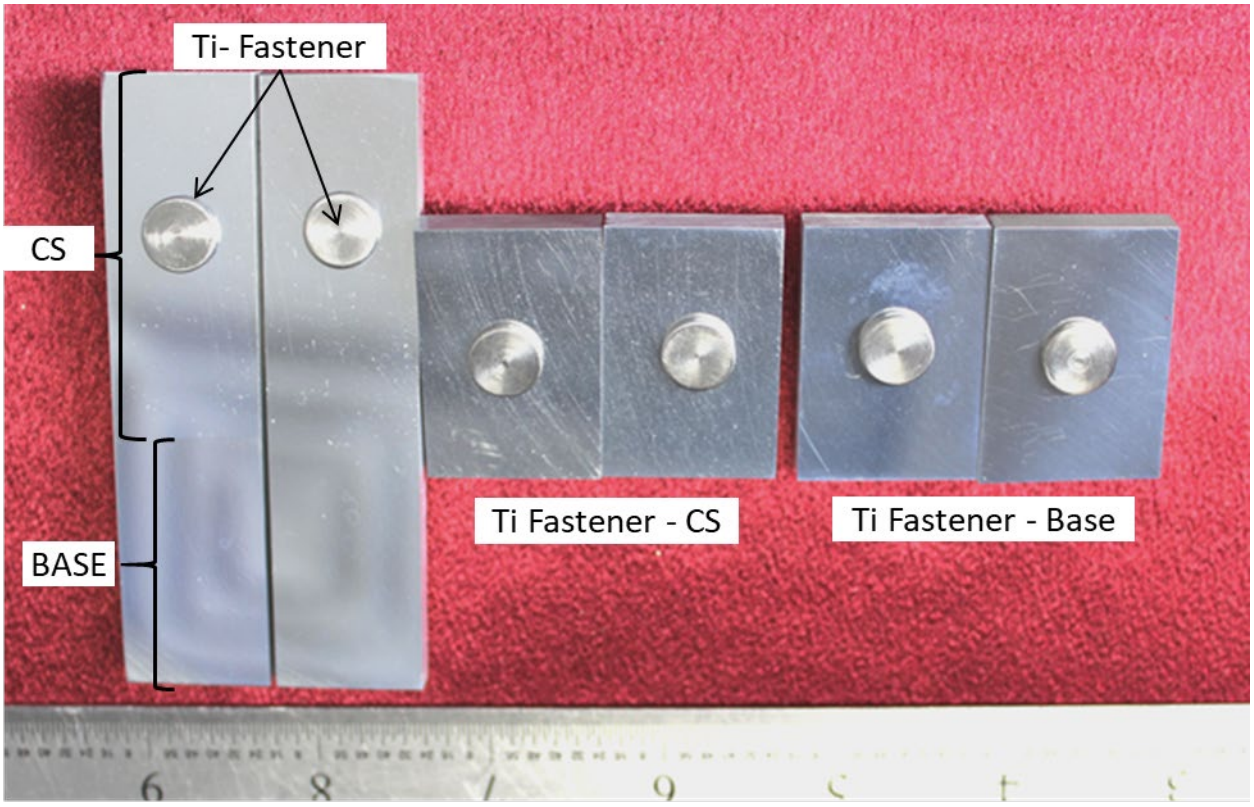

Figure 2. Macrograph showing exfoliation coupons with Ti fasteners installed before exposing to EXCO solution.

3. RESULTS AND DISCUSSION

3.1 Microstructure

Extensive microstructural characterization was carried out to understand the cold sprayed coating. Microstructural observations of the top CS surface show severe deformation with an adiabatic sheared region surrounding some of spherical particles. Low and high magnification optical micrographs of the top surface are shown in Figure 3a and Figure 3b, respectively. Adiabatic shear flow is the most common feature observed in the cross-section view. Figure 3c and Figure 3d show low and high magnification images of the coating cross section. The microstructure of the CS coating in the cross section shows oriented deformed particles defining the spray angle.

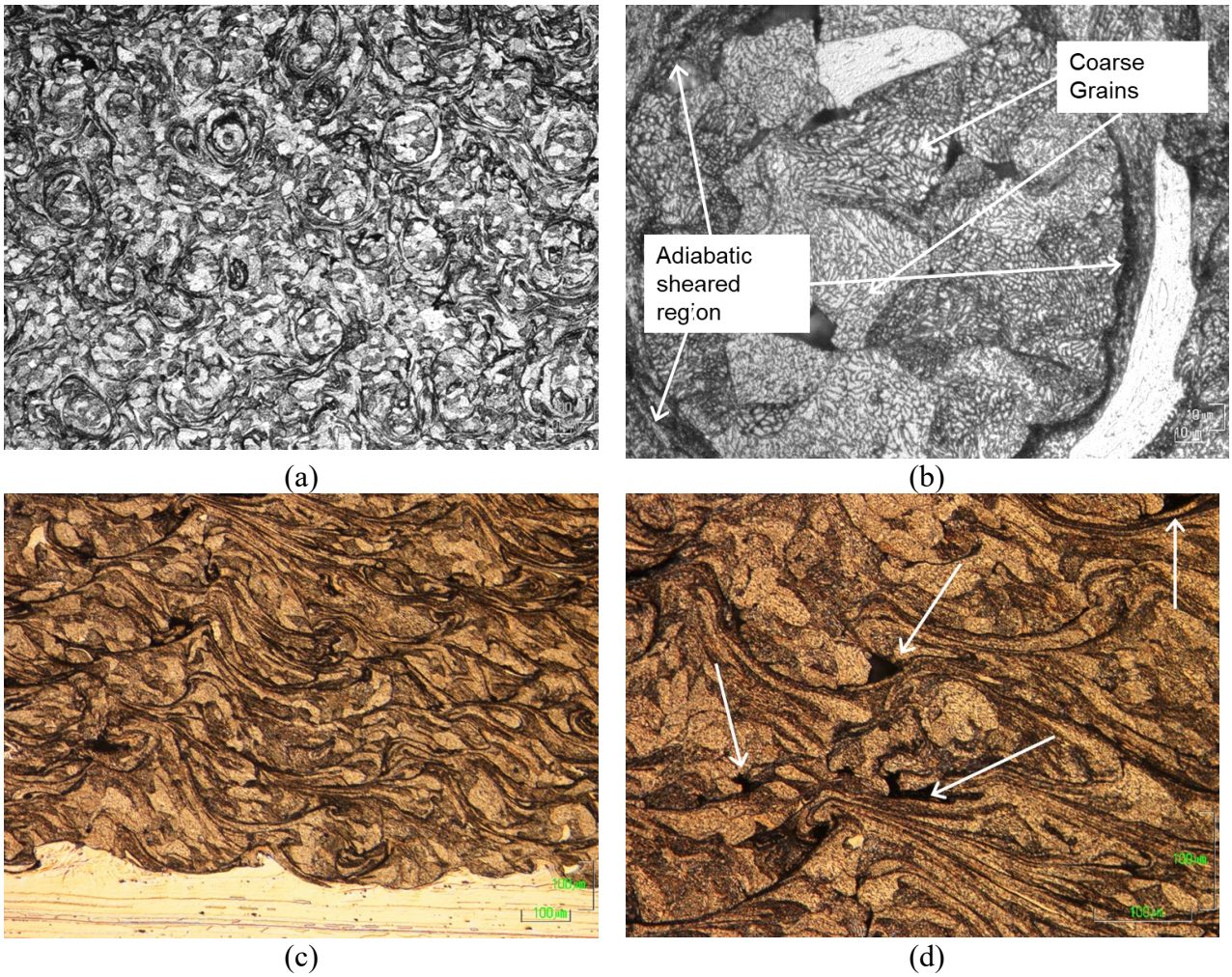

Figure 3. (a) Optical micrograph showing polished and etched microstructure of the top surface of the Al 7075 cold spray coating. (b) Optical micrograph showing higher magnification of the spherical particles with fine dendrites inside coarse grains and adiabatic sheared regions. (c) Optical micrograph showing polished and etched microstructure of the cross section of the CS coating. (d) Optical micrograph showing a higher magnification cross section of the coating with porosity (shown by arrows) at the particle interface.

SEM observation of the top surface shows porosity ranging from 0.7% to 3.8%. Higher percentage porosity is aligned and is related to spray parameter, specifically pitch (Offset). However, the average percentage porosity measured in the cross section was only 0.4%± 0.03. Observation of higher percentage porosity on the top surface indicates further refinement of the spray parameters is required. Figure 4a shows the SEM micrograph of the top surface with the porosity aligned. Despite observed porosity, the interfacial bonding and cohesive bonding between the particles appears to be good, from the SEM observation. Figure 4b shows a representative image of the clean interface that was observed everywhere between the coating and substrate. Similarly, observation of severely deformed particles with adiabatic shear flow is shown in Figure 4c.

Microstructural observations of the adiabatic shear on the top of the cold spray surface as well as in the cross section indicate the spray parameters were optimized for enhanced adhesion and cohesive bonding. The adiabatic shear region represents the particle-particle interface in the CS. Measured diameters of CS particles ranged from 170 to 200 μm indicating that the as received 44 μm particles are severely deformed by the cold spray process. However, observation of aligned porosity does indicate a minor tuning on the offset or pitch spray parameter is required. Furthermore, observation of fine dendrites inside the core of the aluminum powder particles suggest the microstructural characteristics of the as received powders are retained in bulk and the effect of adiabatic deformation is confined to the particle interface.

3.2 Hardness

Nano hardness profiles across the CS and substrate are shown in Figure 5. Hardness distribution in the CS shows a scatter region with a hardness range varying from 98 Vickers Hardness Number (VHN) to 162 VHN. A maximum hardness of 189 VHN occurs just beneath the CS Substrate interface. Hardness then quickly drops to the bulk hardness value of the substrate (174 VHN). Micro hardness measured inside the core of the CS particle shows an average of 99.5±15 VHN. Hardness measured in the adiabatic shear band registered 161.2 ± 17.1VHN. Figure 6a and Figure 6b show the optical micrographs where hardness measurements were taken.

The distribution of microstructural features, i.e., retention of the as received dendritic morphology in the particle core and adiabatic shear in the periphery is reflected in the nano-hardness values. The non-uniform hardness distribution in the CS coating is primarily due to microstructural variation observed in the coating. This is further confirmed by microhardness values measured from pre-defined locations in the CS coating. A substantial increase in the hardness is noted at the particle interface (adiabatic shear region) and is attributed to the increased dislocation density and possibly finer grain size at sheared region. Similar increased hardness behavior near the particle interface has been reported earlier [16, 17].

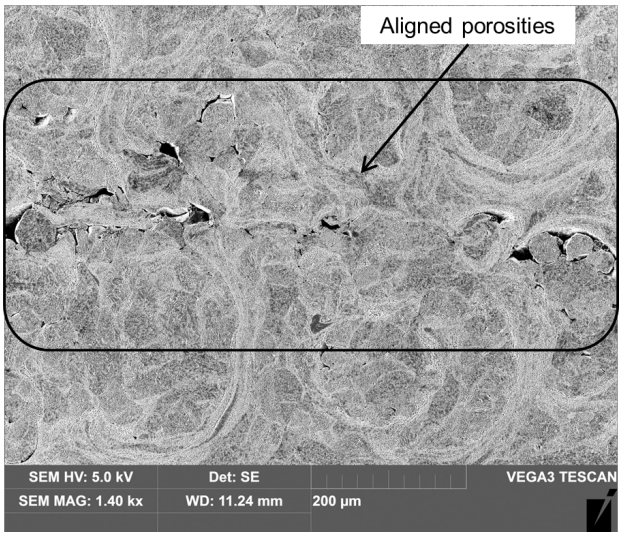

(a)

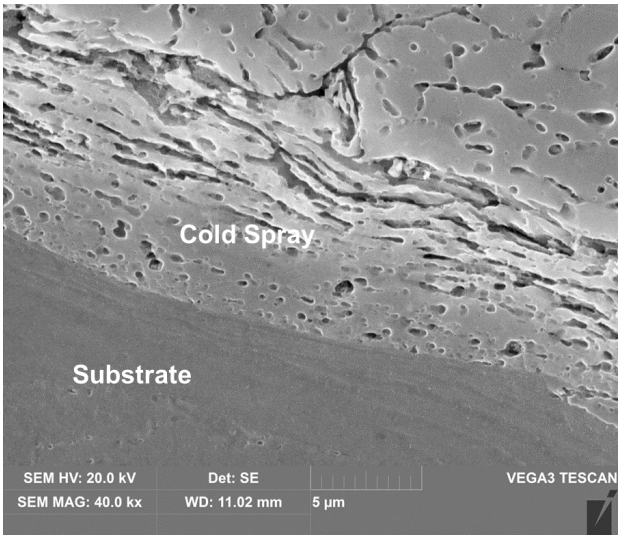

(b)

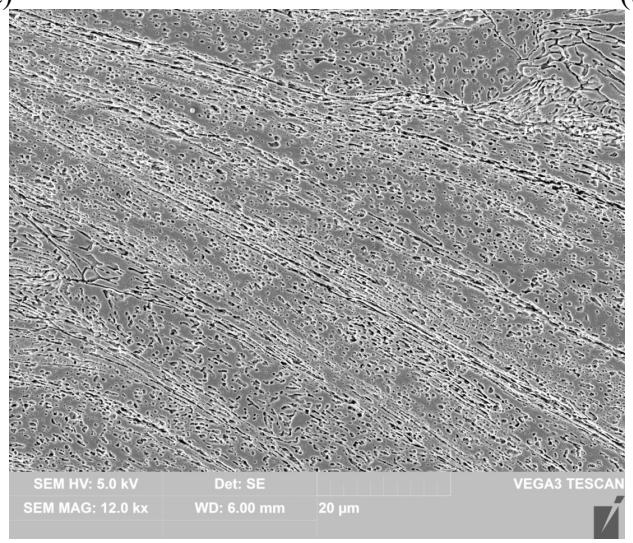

(c)

Figure 4. (a) SEM micrograph showing aligned porosities on the top surface. (b) SEM micrograph showing a clean interface between the particle and the substrate. (c) SEM micrograph showing adiabatic shear flow between the particles. This indicates an increased cohesive strength between particles.

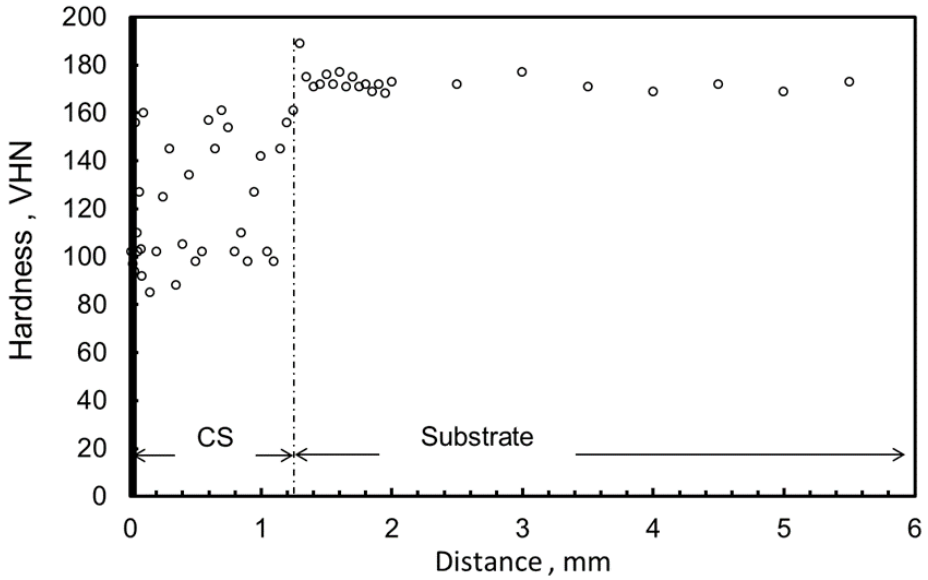

Figure 5. Nano hardness distribution from the top of the Al 7075 CS to the AA7075 T651 substrate.

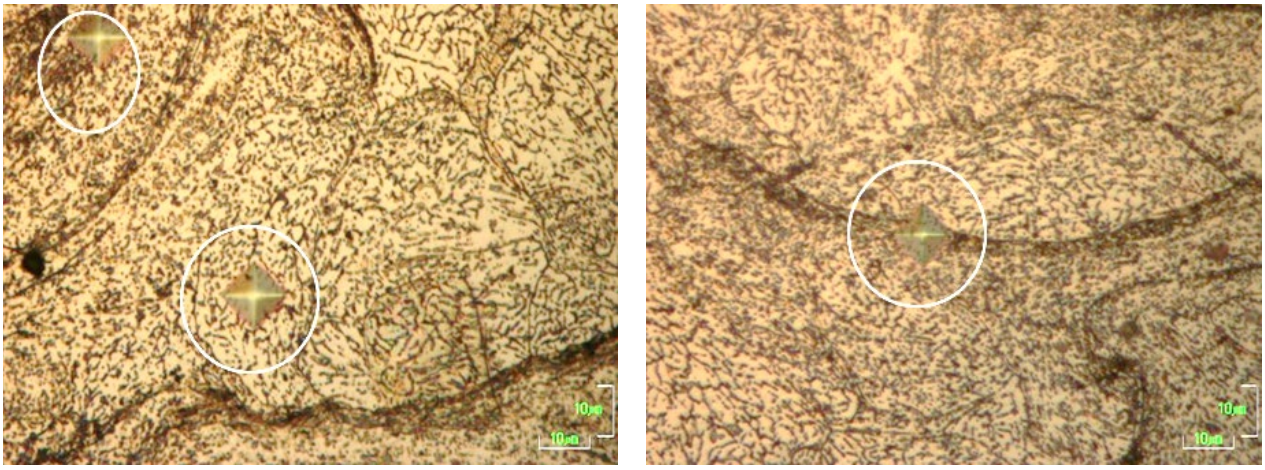

(a) (b)

Figure 6. (a) Micrograph showing indentation location inside the core of the particle. (b) Micrograph showing indentation location at the severely deformed region of the particle.

3.3 Open circuit potential

Prior to the start of the galvanic current testing, the open circuit potential (OCP) is measured for each sample. The results of this testing is shown in Figure 7. As expected based on prior work the CS7075 samples are more electrochemically active than the base AA7075, meaning the CS coating can be used to cathodically protect the base alloy [18]. The potential values are also within 0.1V suggesting that concerns about galvanic corrosion should be limited, but more testing is required to validate these results for service conditions especially given that the Department of the Navy operates in harsh environmental conditions.

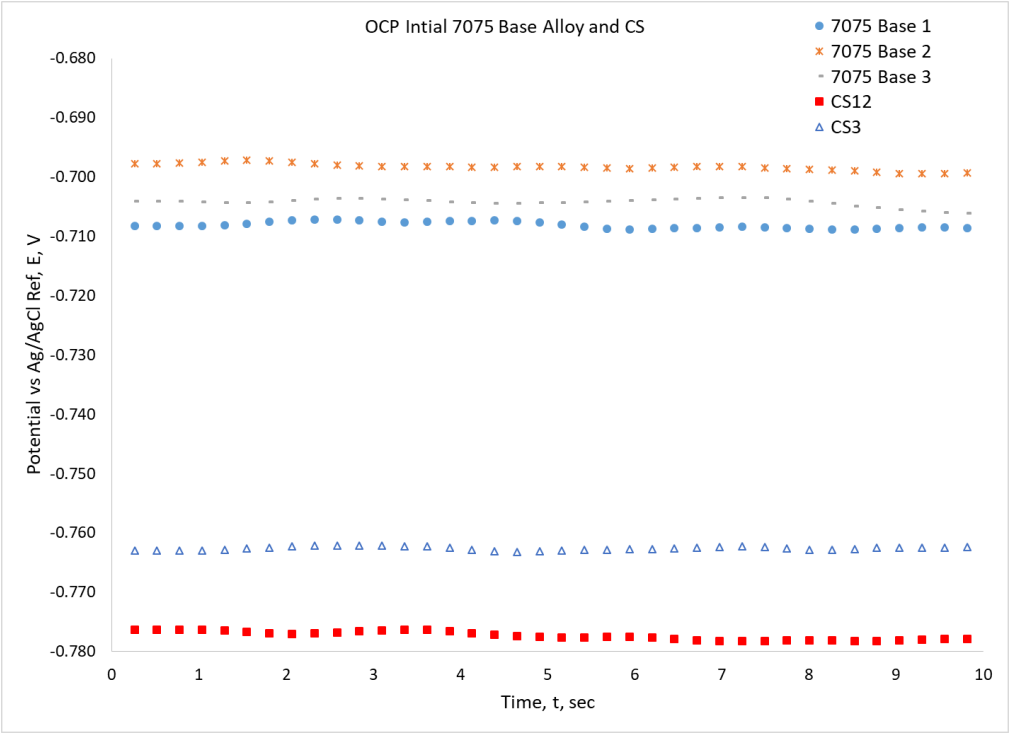

Figure 7. Open circuit potential measured prior to galvanic current testing for three samples of the base AA7075 and two CS7075 samples. The CS is more active than the base material.

3.4 Galvanic current measurement (ASTM G71)

For the galvanic current measurement Figure 8 shows the galvanic current results between the Base-Base and Base-CS parings, each test was run for 48 hours to allow equilibrium to occur. As expected the Base-CS sample has a larger current between the samples almost 15 µA at the highest. However the low overall current value, in µA shows that the galvanic couple between the CS and Base material is only slightly higher than the Base-Base current which is almost 6 µA when the material hit steady state. These results continue to show that the CS will be more electrochemically active than the base aluminum alloy, which is desirable from a repair perspective.

For the galvanic couples with the fastener materials, Figures 9 and 10 show the results. Figure 9 shows the Base-SS304 and CS-SS304 couples. In this case the base material has a higher galvanic current when paired with the stainless steel fastener. This is somewhat surprising as the CS-SS304 couple should have a greater potential difference than the Base-SS304 couple. For the Base-Ti-6Al-4V and CS-Ti-6Al-4V couples shown in Figure 10 the galvanic current is virtually the same for both couples highlighting a limited difference.

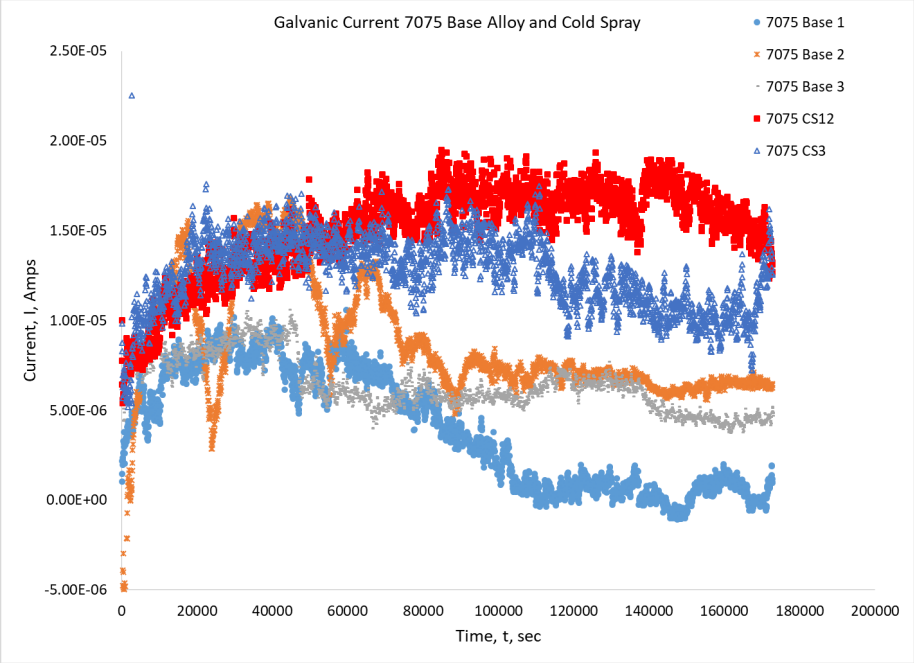

Figure 8. Galvanic current measurements for the Base-Base and Base-CS (noted as CS) material parings.

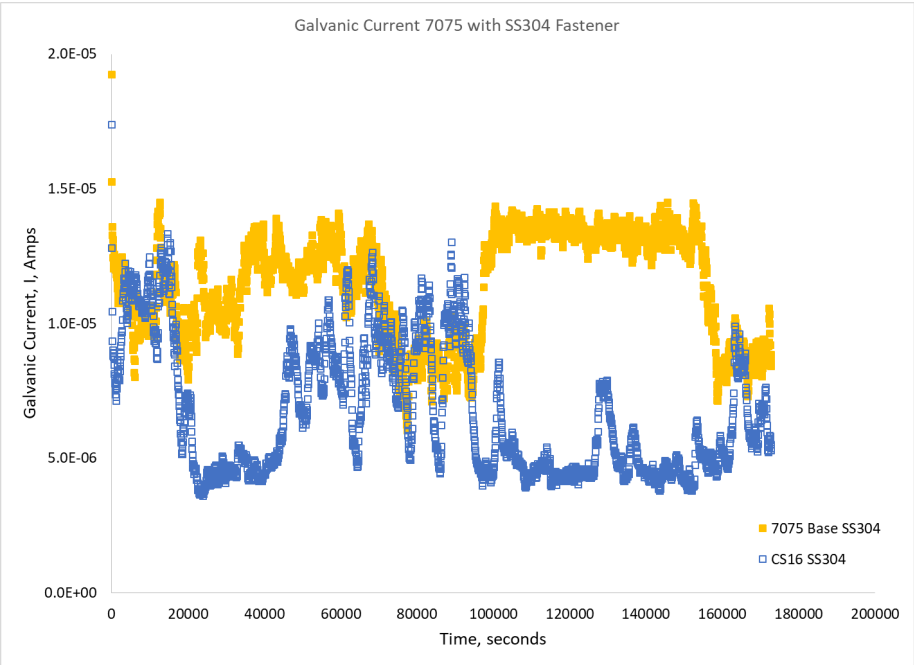

Figure 9. Galvanic current for the Base-SS304 and CS-SS304 material couples in 1 M NaCl.

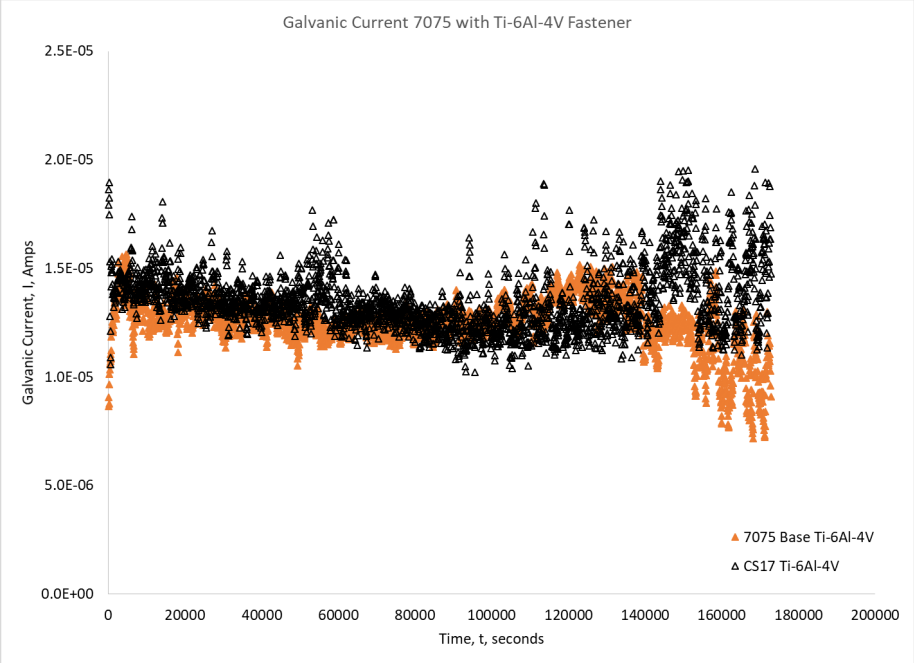

Figure 10. Galvanic current for the Base-Ti-6Al-4V and CS-Ti-6Al-4V material pairs in 1 M NaCl.

3.5 Exfoliation corrosion (ASTM G34)

For the exfoliation testing, each sample was removed from solution after 48 hours and evaluated for exfoliation corrosion damage. The surface condition of each sample with a Ti-6Al-4V fastener is documented in Figure 11 and SS304 Fastener in Figure 12. The G34 ratings system was used and all samples fell within the EC to ED exfoliation damage range, which is expected for AA7075-T651 [14]. The only exception were the combined CS-Base couples. In those cases the Base material was rating was EA while the CS was EC to ED [14]. Figure 11 and Figure 12 show an example of this limited damage for the Base material. For the fastener-Base or fastener-CS combinations, the fastener-Base alloy couple appeared to perform slightly worse (ED versus EC) with respect to surface damage, also shown in Figure 11 and Figure 12. The exfoliation ratings did not vary based on fastener material (SS304 versus Ti-6Al-4V) type.

Post exposure each sample was sectioned, polished and etched. Then the sample cross section was examined to determine how deep the exfoliation damage was and if there was preferential damage around the fastener or the CS-substrate interface. For all of the samples the exfoliation damage was on the sample surface with no preferential damage around the fastener bore, see Figure 13a for an example of a damage free bore with a CS sample with a Ti-6Al-4V fastener. Figure 13b shows the interface between the CS and substrate for a sample with a Ti-6Al-4V fastener, note the surface attack with no preferential undercutting on the base material near the interface. Figure 14 shows a comparison between a Base alloy sample with a SS304 fastener (Figure 14a) and a CS sample with a SS304 fastener (Figure 14b). The cross section evaluation shows little difference in the performance of the CS versus the base substrate when paired with a fastener with all attack limited to the sample surface.

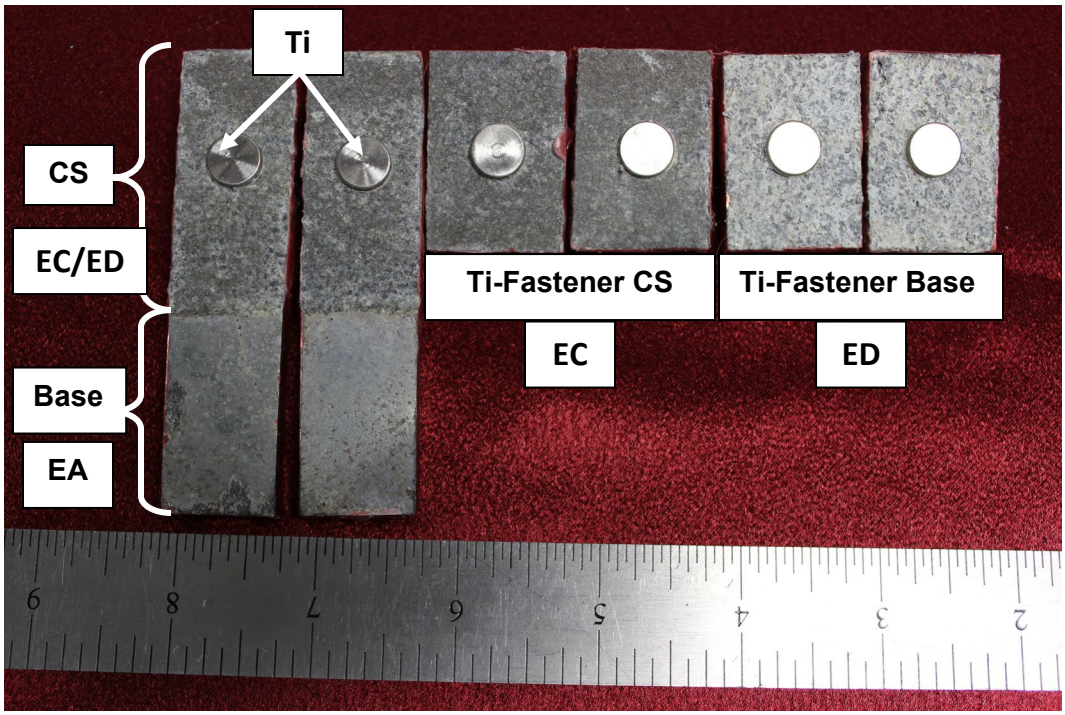

Figure 11. EXCO exposed CS and Base 7075 samples with Ti-6Al-4V fasteners.

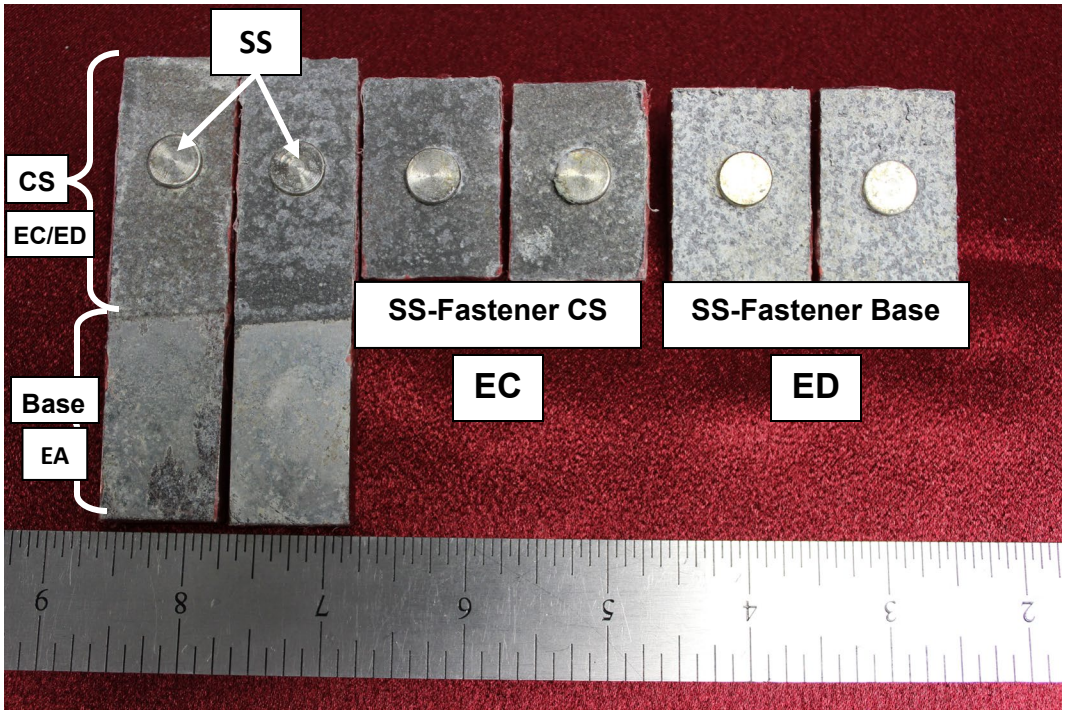

Figure 12. EXCO exposed CS and Base 7075 samples with SS304 fasteners.

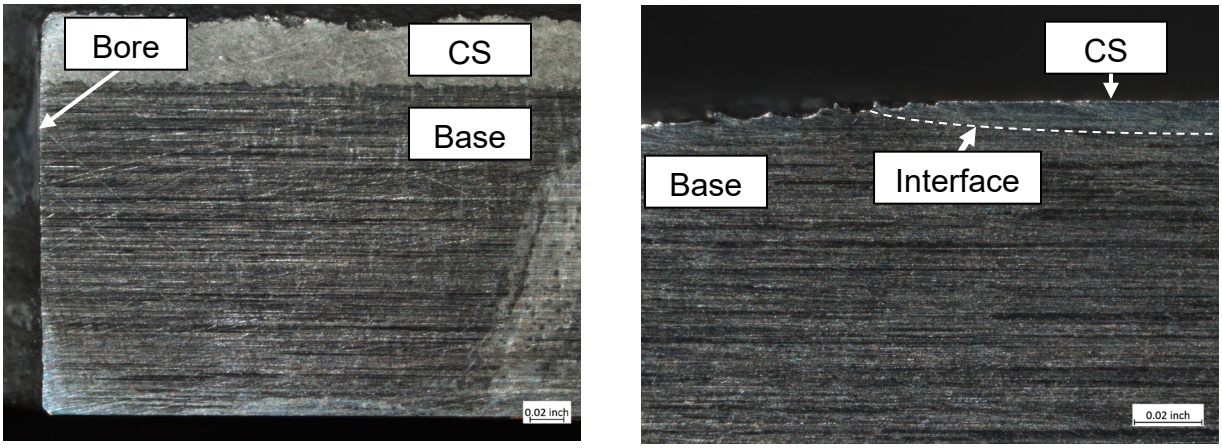

(a) Ti Fastener Cross Section Near Bore

(b) Ti Fastener Cross Section CS-Base Interface

Figure 13. Cross section of samples with Ti fasteners post EXCO exposure.

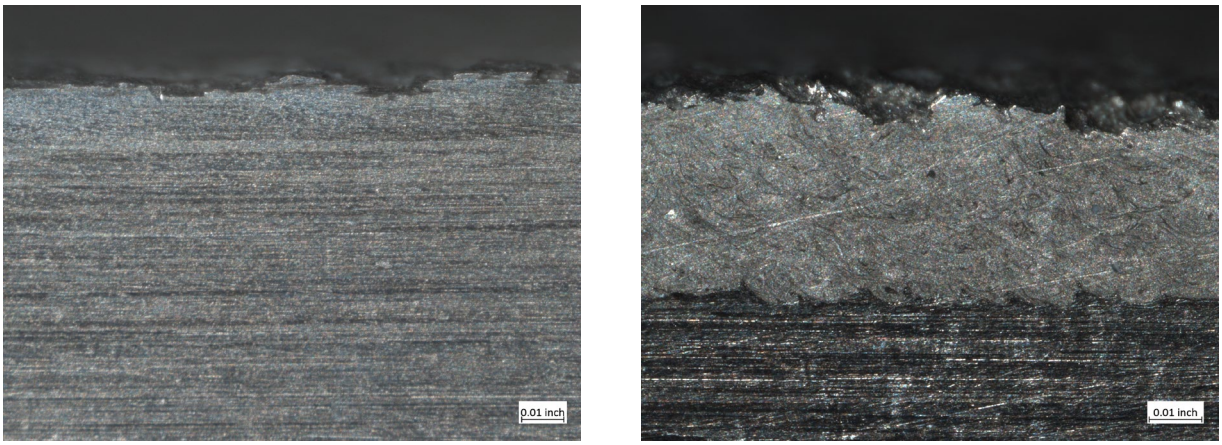

(a) Base AA7075 with SS304 fastener

(b) CS with SS304 fastener

Figure 14. Cross section of samples with SS fasteners post EXCO exposure.

4. CONCLUSIONS

The goal of this program is to provide the Department of the Navy and the DoD with a qualification and approval plan for CS as a structural repair process for sea-based aircraft. To guide this method development an understanding of the critical material properties required and the process control documentation needed is required. Based on prior work the recommended material properties are tensile, fatigue and bearing, in addition to coating characteristics such as percentage porosity, hardness and shear strength. As the operating environment for DoD aircraft can be extreme from a corrosion damage perspective. As such, it is critical to understand how a CS repair will compare to a Base aluminum alloy with respect to corrosion performance. To

begin to document these CS repair properties the microstructure and corrosion performance of a CS repair on 7075-T651 with Al7075 powder was evaluated. It was shown that the CS repair had adiabatic sheared regions, a clean boundary, with good interfacial bonding and cohesive bonding. The porosity was higher and more aligned than desired on the surface. For the electrochemical evaluation it was confirmed that the CS coating is more active than the base alloy, which is a desirable feature from a galvanic standpoint. For the galvanic current testing, as expected, the CS-Base repair has a slightly higher current than the Base-Base pair. During exfoliation testing it was shown that the CS repair performs similarly to the base alloy with either a titanium or stainless steel fastener. However when a CS-Base couple with a fastener is present the CS has corrosion damage similar to the other exfoliation results but the base alloy is protected. This confirms that the CS is protecting the base alloy. No preferential damage around fasteners or at the CS repair interface was noted after the exfoliation exposure. All of these results suggest that CS is a viable repair option, which will not produce unexpected corrosion damage in the substrate material around repaired regions.

5. ACKNOWLEDGEMENTS

This work was funded under United States Air Force Academy (USAFA) Broad Agency Announcements (FA-7000-18-2-0015 and FA7000-14-2-0013) by the Office of Naval Research Science and Technology and the United States Department of Defense, Corrosion Policy and Oversight Office under the Technical Corrosion Collaboration. Research was completed at the United States Air Force Academy Center for Aircraft Structural Life Extension (CAStLE).

The views and conclusions contained herein are those of the authors and should not be interpreted as necessarily representing the official polices and endorsements, either expressed or implied, of the US Air Force Academy, the United States Navy, or the US Government.

6. REFERENCES

1. Moridi, A Hassani-Gangaraj, A.M., Guagliano, M and Dao, M., “Cold spray coating: review of material systems and future perspectives,” *Surface Engineering* 36(6) (2014): 369-395. https://doi.org/10.1179/1743294414Y.0000000270
2. “Efforts to reduce corrosion on the military equipment and infrastructure of the department of defense,” United States office of the Secretory of Defense, USA, Department of Defense, (2007).
3. Karthikeyan J., “Cold Spray Technology: International Status and USA Efforts.” *ASB Industries*, (2004): 1-14.
4. Decker M. K. and Smith M. F., “Thermal and Cold Spray Analysis of Density, Porosity and Tensile Specimens for Use with LIGA Applications,” SAND2000-0339, Sandia National Laboratories, (2000). DOI: 10.2172/752018
5. Startwell B. D., Kestler R., Legg K. O., Assink W., Nardi A., Sichell J., “Validation of HVOF WC/Co, WC/CoCr and Tribology 800 Thermal Spray Coatings as a Replacement For Hard Chrome Plating On C-2/E-2/P-3 and C-130 Propeller Hub System Components,” NRL-PP-99-22-FR-01, Naval Research Laboratory, Washington: (2003).

6. Sakaki K, “Cold Spray Process Overview and Application Trends,” *Mater Science. Forum* (2004), 449-452: 1305-8.
7. Karthikeyan J., “Development of Oxidation Resistant Coatings on Grcop-84 Substrates By Cold Spray Process,” NASA-CR 2007-214706 (2007).
8. Pepi M., “Cold Spray Technology for Repair of Magnesium Rotorcraft Components,” *NAVAIR Corrosion Resistant Alloy Workshop*: (2006).
9. Villafuerte J., “Current and Future Applications of Cold Spray Technology, Recent Trends in Cold Spray Technology: Potential Applications for Repair of Military Hardware,” NATO RT-MP-AVT-163 (2010):1-14.
10. Matthews N., at al “Supersonic Particle Deposition (SPD) Cutting Edge Technology for Corrosion Protection and Damaged Metallic Component Recover in: *Proceedings 2010 SDE Symposium Program “Design Engineering in SRP Environment* (2010). https://doi.org/10.1016/j.ijfatigue.2011.03.013
11. Stoltenhoff T. “Praxair Surface Technologies” *8th Colloquium, HVOF Spraying Cold Spray, Conference*, (2009).
12. Dykhuizen, R.C., Smith, M.F., Gilmore, D.L., Neiser, R.A., Jiang, X. and Sampath, S. “Impact of high velocity cold spray particles:, *J. Thermal Spray Technol.*, 8 (1999): 559–564. https://doi.org/10.1361/105996399770350250
13. ASTM Standard B117-18, 2018, “Standard Test Method for Operating Salt Spray (Fog) Apparatus” ASTM International, West Conshohocken, PA. DOI: 10.1520/B0117-18, www.astm.org.
14. ASTM Standard G34-01, 2018, “Standard Test Method for Exfoliation Corrosion Susceptibility in 2XXX and 7XXX Series Aluminum Alloys (EXCO Test),” ASTM International, West Conshohocken, PA. DOI: 10.1520/G0034-01R18, www.astm.org.
15. ASTM Standard G71-81, 2014, “Standard Test Method for Conducting and Evaluating Galvanic Corrosion Tests in Electrolytes”, ASTM International, West Conshohocken, PA. DOI: 10.1520/G0071-81R14, www.astm.org.
16. Rokni, M.R., Widener, C.A., Crawford, G.A. West, M.K. “An investigation into microstructure and mechanical properties of cold sprayed 7075 Al deposition”, *Mater. Sci. Eng*. *A*. 625 (2015):19-27, https://doi.org/10.1016/j.msea.2014.11.059
17. Zou, Y., Goldbaum, D.., Szpunar, G.A, Yue, S: “Microstructure and nanohardness of cold-sprayed coatings: Electron backscatter diffraction and nanoindentation studies”, *Scr. Mater.* 62(6) (2010): 395-398. https://doi.org/10.1016/j.scriptamat.2009.11.034
18. Galyon Dorman, S.E, Niebuhr, J.H, Arunachalam, S.R., Buckley, R.T. and Fawaz, S.A. “Predicting and Managing Atmospheric Corrosion in DOD High Strength Aluminum Alloys.” *SAFE Inc* SAFE-RTP-17-032 (2018).